Author Manuscript

Author Manuscript

Author Manuscript

Author Manuscript

HHS Public Access

Author manuscript

*Org Biomol Chem*. Author manuscript; available in PMC 2017 October 17.

Published in final edited form as:

*Org Biomol Chem*. 2014 July 21; 12(27): 4872–4878. doi:10.1039/c4ob00745j.

# Rare *Streptomyces* sp. polyketides as modulators of K-Ras localisation†

**Angela A. Salim**[‡,a], **Xue Xiao**[‡,a], **Kwang-Jin Cho**[b], **Andrew M. Piggott**[§,a], **Ernest Lacey**[c], **John F. Hancock**[b], and **Robert J. Capon**[*,a]

[a]Institute for Molecular Bioscience, The University of Queensland, St. Lucia, QLD 4072, Australia

[b]Integrative Biology and Pharmacology, The University of Texas Medical School, Houston, Texas 77030, USA

[c]Microbial Screening Technologies Pty. Ltd, Building C, 28-54 Percival Rd., Smithfield, NSW 2164, Australia

## Abstract

Chemical investigations of a soil-derived Streptomyces sp. led to the isolation of five new polyketides, (+)-oxanthromicin, (±)-*hemi*-oxanthromicins A/B, (±)-*spiro*-oxanthromicin A and oxanthroquinone, and the known alkaloid staurosporine, and the detection of four new metastable analogues, (±)-*spiro*-oxanthromicins B1/B2/C1/C2. Among the compounds tested, SAR investigations established that the synthetic oxanthroquinone ethyl ester and 3-*O*-methyl-oxanthroquinone ethyl ester were optimal at mislocalising oncogenic mutant K-Ras from the plasma membrane of intact Madin-Darby canine kidney (MDCK) cells ($IC_{50}$ 4.6 and 1.2 μM), while a sub-$EC_{50}$ dose of (±)-*spiro*-oxanthromicin A was optimal at potentiating (750%) the K-Ras inhibitory activity of staurosporine ($IC_{50}$ 60 pM). These studies demonstrate that a rare class of *Streptomyces* polyketide modulates K-Ras plasma membrane localisation, with implications for the future treatment of K-Ras dependent cancers.

## Introduction

Ras GTPases are key molecular switches that regulate cell growth, proliferation and differentiation, and are ubiquitously expressed in mammalian cells as three isoforms (H-Ras, N-Ras and K-Ras).[1] Constitutively activated oncogenic K-Ras is a key driver of oncogenesis in pancreatic adenocarcinomas (95%), colon adenomas (40%) and non-small cell lung cancer (15–20%).[2] The key role played by K-Ras in these cancers is evidenced by experimental data, which demonstrate that inhibition of K-Ras membrane localisation blocks all oncogenic activity.[3] Despite K-Ras inhibitors being very attractive prospects as cancer chemotherapeutics, the development of clinically useful inhibitors has proved elusive.

†Electronic supplementary information (ESI) available: General experimental details, full details of microbial collection and taxonomy, tabulated 2D NMR data and NMR spectra and LCMS stability studies. See DOI: 10.1039/c4ob00745j

Robert J. Capon: r.capon@uq.edu.au; Fax: +61-7-3346-2090; Tel: +61-7-3346-2979.

‡These two authors contributed equally to this paper.

§Present address: Department of Chemistry and Biomolecular Sciences, Macquarie University, NSW 2109, Australia.

Author Manuscript Author Manuscript Author Manuscript Author Manuscript

In an effort to address this challenge, we employed a high-throughput, high-content assay to screen a library of microbial extracts, successfully detecting a *Streptomyces* sp. (MST-134270), isolated from a soil sample collected near Pamplona, Spain, as a source of metabolites that selectively mislocalised Ras proteins. In an earlier report,[4] we described staurosporine (**10**) isolated from this culture as a potent and selective inhibitor of K-Ras plasma membrane (PM) localisation, disrupting phosphatidylserine trafficking at concentrations below the threshold required for high affinity pan-kinase activity. This report extends our earlier findings, to describe the spectroscopic analysis, chemistry and biology of compounds **1**–**9** (Fig. 1), including commentary on their biosynthetic origins, chemical stability and total synthesis.

## Results and discussion

Bioassay-guided fractionation of a solid phase (cracked wheat) cultivation of MST-134270 resulted in the isolation and characterisation of five new polyketides, (+)-oxanthromicin (**1**), (±)-*hemi*-oxanthromicin A (**2**), (±)-*hemi*-oxanthromicin B (**3**), (±)-*spiro*-oxanthromicin A (**4**), and oxanthroquinone (**9**), as well as the detection and identification of four new metastable analogues, (±)-*spiro*-oxanthromicins B1/B2 (**5**/**6**), and (±)-*spiro*-oxanthromicins C1/C2 (**7**/**8**), and the isolation of the known indole alkaloid staurosporine (**10**) (Fig. 1).

HRESI(−)MS measurements on **1** established a molecular formula of $C_{36}H_{30}O_{12}$ (Δmmu −0.2) while the NMR (DMSO-$d_6$) data (Fig. 2 and ESI Table S1a†) revealed only 18 carbon resonances, necessitating a degree of symmetry. Further analysis of the $^1$H NMR data revealed resonances for one tertiary methyl ($\delta_H$ 1.44), two benzylic methyls ($\delta_H$ 2.18 and 2.69), one isolated ($\delta_H$ 7.16) and two *ortho* coupled ($\delta_H$ 6.33 and 7.12, 7.8 Hz) aromatic protons, and a chelated hydroxy group ($\delta_H$ 13.46, s), with diagnostic 2D NMR correlations permitting assembly of a dimeric anthrone featuring a rare peroxide bridge. A search of the literature and comparison of NMR data with the published compound (ESI Table S1b†) confirmed that **1** was (+)-oxanthromicin ($[\alpha]_D^{22}+157$, *c* 0.26, EtOH), a new enantiomer of the rare *Streptomyces* metabolite (−)-oxanthromicin ($[\alpha]_D^{26}-172$, *c* 0.3, EtOH).[5]

Molecular formulae attributed to **2** ($C_{18}H_{16}O_6$, Δmmu +0.8) and **3** ($C_{19}H_{18}O_6$, Δmmu −0.2) on the basis of HRESI(−)MS measurements were suggestive that both compounds contain the monomer polyketide unit in **1**. Supportive of this hypothesis, analysis of the NMR (DMSO-$d_6$) data for **2** and **3** (Fig. 2 and ESI Tables S2–S3†) revealed differences centred around replacement of the C-10 peroxy bridge in **1** with (i) a 10-OH ($\delta_H$ 6.11) moiety in **2**, exhibiting HMBC correlations to C-4a, C-10 and C-10a and ROESY correlations to H-4 and H-5, and (ii) a 10-OMe ($\delta_H$ 2.81, s; $\delta_C$ 51.8) moiety in **3**, exhibiting HMBC correlations to C-10 and ROESY correlations to H-4 and H-5. These observations, together with the lack of an optical rotation, permitted assignment of racemic structures to (±)-*hemi*-oxanthromicins A (**2**) and B (**3**) as indicated. Similarly, HRESI(−)MS measurements on **9** ($C_{17}H_{12}O_6$,

†Electronic supplementary information (ESI) available: General experimental details, full details of microbial collection and taxonomy, tabulated 2D NMR data and NMR spectra and LCMS stability studies. See DOI: 10.1039/c4ob00745j

Author Manuscript Author Manuscript Author Manuscript Author Manuscript

Δmmu +0.7) together with analysis of the 1D and 2D NMR (DMSO-$d_6$) data (Fig. 2 and ESI Table S5†) permitted assignment of the structure for oxanthroquinone (**9**) as indicated.

HRESI(−)MS measurements established a molecular formula of $C_{36}H_{26}O_{10}$ (Δmmu −0.3) for **4**, while analysis of the NMR (DMSO-$d_6$) data (Fig. 3 and ESI Table S4†), suggested a heavily substituted aromatic system possessing many structural characteristics in common with the co-metabolites **1**–**3**. Detailed analysis of these NMR data, including consideration of diagnostic 2D NMR correlations, permitted assembly of the planar structure as indicated. More specifically, HMBC correlations required that the aromatic methyl $H_3$-13 be flanked by H-6 and the phenolic 8-OH, while additional correlations linked this fragment to the quaternary aromatics C-8a and C-10a, and the $sp^3$ *spiro* C-10′. COSY correlations established the $H_2$-14′ to H-14 fragment, while HMBC correlations linked this fragment to C-10′, C-5, C-10a and C-10. Further HMBC correlations required that the aromatic methyl $H_3$-11 be flanked by C-2 and C-9a, and *para*-disposed to H-4, which was in turn flanked by C-4a and C-5 (the latter bearing a hydroxy group). Additional HMBC correlations from H-4 to C-10, supported by ROESY correlations between (i) H-6 and $H_3$-13, (ii) $H_3$-13 and 8-OH, (iii) 8-OH and $H_3$-11 and (iv) H-4 and H-14, defined the ABCD ring system as indicated (Fig. 3). Comparable 2D NMR correlations defined the EFG ring system, with diagnostic HMBC correlations linking the *spiro* C-10′ to H-4′, H-5′ and H-6′. ROESY correlations between H-5′ and both H-6 and $H_2$-14′, and between H-4′ and both H-6 and $H_2$-14′, defined the orthogonal relationship between the ABCD and EFG ring systems (Fig. 3). Despite the presence of a chiral centre (C-10′), the lack of an optical rotation required that (±)-*spiro*-oxanthromicin A (**4**) be assigned the racemic structure as indicated. Further chemical studies supportive of this structure assignment are presented below.

HPLC-DAD-MS analysis of the crude MeOH extract of *Streptomyces* sp. MST-134270 confirmed the dominant cultivation/biosynthetic products as **1**, **2** and **10**, with **3** and **4** only detected at trace levels (ESI Fig. S10†). Significantly, during SPE fractionation, the detected (and recovered) yields of **3** and **4** increased, as did levels of two hitherto undetected compounds **5** and **6**. These observations strongly suggested that **3**–**6** were capable of being produced during handling (ESI Fig. S11†). In support of this hypothesis, exposure of a pure sample of **2** to 0.1% TFA–MeOH (conditions comparable to those encountered during SPE fractionation) resulted in partial conversion to **3** and **4**, while exposure to 0.1% TFA–MeCN yielded only **4** (ESI Fig. S12†). Likewise, a pure sample of **3** was observed to undergo partial conversion to **2** during routine handling.

In an effort to assign structures to **5** and **6**, we noted that their UV-vis (DAD) spectra were similar to those of **1**–**3**, suggestive of closely related chromophores and molecular structures, while HPLC-HRESI(−)MS analysis suggested that **5** ($C_{37}H_{30}O_{11}$, Δmmu +2.4) and **6** ($C_{37}H_{30}O_{11}$, Δmmu +2.0) were isomeric MeOH adducts of **4**. Attempts at purification of **5** and **6** by reversed phase HPLC proved problematic as immediately post-elution both underwent partial conversion to **7** and **8**, a transformation that proceeded to near-completion after standing at r.t. for 3 h (ESI Fig. S13–S14†). The transformation products **7** and **8** exhibited almost identical UV-vis (DAD) spectra to **5** and **6**, with HPLC-HRESI(−)MS analysis suggesting that **7** ($C_{36}H_{28}O_{11}$, Δmmu +0.6) and **8** ($C_{36}H_{28}O_{11}$, Δmmu +0.0) were

Author Manuscript Author Manuscript Author Manuscript Author Manuscript

isomeric $H_2O$ adducts of **4**. On concentrating *in vacuo* and resuspending in MeOH, the mixture of **7** and **8** rapidly transformed to a complex mixture of **4**–**8**, dominated by **4**.

In presenting a plausible mechanism for the biosynthetic/chemical origins of **1**–**9** (Fig. 4), we speculate that the polyketide precursor, oxanthroquinone (**9**), undergoes stereospecific methylation to a single (10*R*) enantiomer of **2**, which in turn undergoes dimerisation to (+)-oxanthromicin (**1**). Acid-mediated dehydration of **2** could deliver an achiral carbocation intermediate that is reversibly quenched with either $H_2O$ or MeOH to yield (±)-*hemi*-oxanthromicin A (**2**) or B (**3**) respectively. Significantly, the carbocation intermediate could also transform, *via* a mechanism foreshadowed in a 1979 study directed at the acid-mediated dimerisation of 10-methyleneanthrone,[6] to yield a (±)-*spiro*-carbocation. The (±)-*spiro*-carbocation could in turn undergo reversible quenching with either MeOH or $H_2O$ to deliver the diastereomeric (±)-*spiro*-oxanthromicin B1 (**5**) and B2 (**6**), or the diastereomeric (±)-*spiro*-oxanthromicin C1 (**7**) and C2 (**8**), respectively. Finally, the acid-labile doubly benzylic 10-OH moiety in **7** and **8** can undergo irreversible dehydration to yield (±)-*spiro*-oxanthromicin A (**4**) as a stable quinone methide. In addition to rationalising the biosynthetic/chemical relationships between **1**–**9**, this biosynthetic/chemical pathway demonstrates for the first time that a rare *spiro* dimerisation mechanism, first proposed in 1979,[6] has a footprint in the natural world.

To support the structural assignments outlined above, and to provide material for a structure activity relationship (SAR) study, we embarked on the syntheses summarised in Scheme 1. Commercially available 2,4-dichloro-1,4-benzoquinone was treated with the Danishefsky diene derived from tiglic aldehyde[7] to form a Diels–Alder adduct, which on Jones oxidation yielded 2-chloro-8-hydroxy-7-methylnaphthaquinone[8] (60%). A subsequent Diels–Alder reaction with the Danishefsky diene derived from ethyl diacetoacetate[9] yielded oxanthroquinone ethyl ester (**11**) (58%) (ESI Fig. S6a–S6b†), which on hydrolysis returned oxanthroquinone (**9**) (88%). Treatment of synthetic **9** with MeMgBr resulted in regioselective addition to C-10 in preference to C-9, which is chelated to the adjacent 8-hydroxy, to yield (±)-*hemi*-oxanthromicin A (**2**) (45%). NMR data showed that synthetic samples **9** and **2** are identical in all respects to the natural products. As the stability studies discussed above had established a sequence of chemical transformations from **2** to **3**–**8**, the total synthesis of **9** and **2** represents a formal synthesis of **3**–**8**. To further explore SAR, we exploited the chelation of 8-OH to selectively mono-methylate **11** with MeI (Scheme 1) to yield 3-*O*-methyl oxanthroquinone ethyl ester (**14**) (72%) (ESI Fig. S7a–S7b†).

On reviewing the polyketide natural products literature, we noted **1**–**9** possess unique 1-Me/7-Me and 2-$CO_2H$ substitutions. To explore the possible SAR significance of the 7-Me and 2-$CO_2H$ moieties, we completed the syntheses outlined in Scheme 2, transforming 3-bromojuglone to 7-desmethylox-anthroquinone ethyl ester (**12**) (68%) (ESI Fig. S8a–S8b†) and 7-desmethyloxanthroquinone (**13**) (90%) (ESI Fig. S9a–S9b†).

We next set out to use quantitative confocal imaging to measure the ability of **1**–**2**, **4**, **9** and **11**–**14** to mislocalise oncogenic mutant K-Ras (mGFP-K-RasG12 V) from the PM of intact Madin-Darby canine kidney (MDCK) cells following a previously published protocol.[4] The results (Table 1) revealed that the natural product (+)-oxanthromicin (**1**), the dimeric

Author Manuscript Author Manuscript Author Manuscript Author Manuscript

transformation product (±)-*spiro*-oxanthromicin A (**4**) and the synthetic ethyl ester analogues **12**, **11** and **14** (in increasing order of potency) were effective at mislocalising K-Ras from the PM. An SAR analysis of these data suggests that the monomers **11** and **12**–**14** are more active than the dimers **1** and **4**, and that esterification of the 2-$CO_2H$ moiety improves K-Ras mislocalisation. Activity is further enhanced by the presence of a 7-Me, and substitution (methylation) of the 3-OH.

To further our investigations into oxanthromicin/oxanthroquinone chemistry and biology, we analysed our in-house database of the HPLC-DAD secondary metabolite profiles of ~50 000 microbial extracts, to detect additional *Streptomyces* capable of producing examples of this structure class. This study revealed two *Streptomyces* that were subsequently re-cultivated and subjected to detailed chemical analysis. *Streptomyces* sp. MST-RA9773 isolated from a soil sample collected near Barellan, New South Wales (NSW), and *Streptomyces* sp. MST-104069 isolated from a soil sample collected near Broken Hill, NSW, produced **1** and related *hemi*- and *spiro*-oxanthromicins, only the former produced **10**. This analysis established that oxanthromicins/oxanthroquinone are exceptionally rare with an incidence (in our library) of ~1 : 17 000, in contrast to staurosporine with an incidence of ~1 : 100. The repeated co-production of oxanthromicins/oxanthroquinone and staurosporine is noteworthy, and raised the possibility that these structurally diverse microbial metabolites may exhibit synergistic biological properties. To probe this hypothesis, we quantified the K-Ras mislocalising properties of **10** when exposed to sub-$IC_{50}$ doses of **1**–**2**, **4**, **9** or **12**–**13** (4 μM), **11** (1.45 μM) and **14** (0.60 μM), revealing significant levels of synergism by **1** (130%), **4** (750%), **11** (410%) and **14** (470%).

## Conclusions

In conclusion, this report describes a successful high-throughput, high-content microbial biodiscovery approach to detect and identify novel small molecule inducers of K-Ras PM mislocalisation. Our chemical investigations of *Streptomyces* sp. MST-134270 yielded a suite of new polyketides **1**–**9**, interconnected by an array of biosynthetic and chemical transformations, inclusive of the first natural occurrence of a rare *spiro* dimerisation reaction. Structure elucidations were supported by detailed spectroscopic analysis, chemical interconversion and total synthesis. SAR studies established the synthetic anthraquinone **14** as a potent lead candidate, capable of mislocalising oncogenic mutant K-Ras (mGFP-K-RasG12 V) from the PM of intact MDCK cells. We established the natural occurrence of oxanthromicins/oxanthroquinone (in our library) as being exceptionally low, and correlated with the co-production of staurosporine (**10**). Co-treatment of **10** with sub-$EC_{50}$ doses of selected oxanthroquinones resulted in a significant synergism of K-Ras PM mislocalisation. Collectively, these studies demonstrate that a rare class of *Streptomyces* polyketides, and analogues inspired by these compounds, can induce significant K-Ras PM mislocalisation ($IC_{50}$ 1.2 μM), and can synergise the K-Ras PM mislocalisation properties of staurosporine ($IC_{50}$ 60 pM). A detailed account of the biological properties and mechanism of action of these polyketides will be reported elsewhere.

Author Manuscript Author Manuscript Author Manuscript Author Manuscript

## Experimental section

### Microbial cultivation and extraction

A *Streptomyces* sp. (MST-134270) cultivation was incubated for 10 days at 28 °C in 40 Erlenmeyer flasks (250 mL each) containing sterilised cracked wheat (50 g) hydrated in water (30 mL), and inoculated with 5 mL of a ISP2 media seed fermentation. The resulting ferment (3.14 kg) was extracted with acetone (6 L), filtered and concentrated *in vacuo* to an aqueous concentrate (800 mL). The aqueous concentrate was extracted with EtOAc (1.5 L) and concentrated *in vacuo* to yield a crude EtOAc extract (7.2 g), which was subsequently partitioned between hexane and MeOH to give hexane-soluble (2.4 g) and MeOH-soluble (4.8 g) extracts (ESI Scheme S1†).

### Fractionation and characterisation of compounds

A portion of MeOH-soluble extract (206 mg) was fractionated using a $C_{18}$-max SPE cartridge (5 g) eluting with a stepwise gradient from 90% $H_2O$–MeOH to 100% MeOH with isocratic 0.01% TFA modifier to give Fractions A–G. SPE Fraction E (62 mg), eluting at 30% $H_2O$–MeOH, was further fractionated by semi-preparative HPLC (Agilent Zorbax XDB-$C_8$, 5 μm, 9.4 × 250 mm column, 10 min gradient elution at 3.5 mL $min^{-1}$ from 70–20% $H_2O$–MeCN, then 100% MeCN for 5 min, with isocratic 0.01% TFA modifier) to afford staurosporine (**10**) ($t_R$ 4.8 min, 16.0 mg), (±)-*hemi*-oxanthromicin A (**2**) ($t_R$ 8.1 min, 17.1 mg) and (±)-*hemi*-oxanthromicin B (**3**) ($t_R$ 10.1 min, 2.9 mg). SPE Fraction F (40 mg), eluting at 15% $H_2O$–MeOH, was further fractionated by semi-preparative HPLC (Agilent Zorbax XDB-$C_8$, 5 μm, 9.4 × 250 mm column, 12 min gradient elution at 3.5 mL $min^{-1}$, from 50–20% $H_2O$–MeCN with isocratic 0.01% TFA modifier) to afford staurosporine (**10**) ($t_R$ 2.8 min, 7.5 mg), (±)-*hemi*-oxanthromicin A (**2**) ($t_R$ 5.2 min, 8.0 mg), oxanthroquinone (**9**) ($t_R$ 6.5 min, 2.0 mg), (±)-*hemi*-oxanthromicin B (**3**) ($t_R$ 7.5 min, 5.1 mg), (±)-*spiro*-oxanthromicin B1 (**5**)* ($t_R$ 9.0 min, 2.0 mg), (±)-*spiro*-oxanthromicin A (**4**) ($t_R$ 9.8 min, 1.8 mg), (±)-*spiro*-oxanthromicin B2 (**6**)* ($t_R$ 10.6 min, 1.5 mg). (*Note: **5** and **6** transformed to the more stable 4 during the removal of HPLC solvents.) SPE Fraction G (55 mg), eluting with MeOH, was further fractionated by semi-preparative HPLC (Agilent Zorbax XDB-$C_8$, 5 μm, 9.4 × 250 mm column, 12 min gradient elution at 3.5 mL $min^{-1}$, from 60% $H_2O$–MeCN to 100% MeCN with isocratic 0.01% TFA modifier) to afford staurosporine (**10**) ($t_R$ 3.5 min, 5.5 mg), (±)-*hemi*-oxanthromicin A (**2**) ($t_R$ 6.2 min, 0.7 mg), (±)-*hemi*-oxanthromicin B (**3**) ($t_R$ 8.2 min, 1.8 mg), (±)-*spiro*-oxanthromicin A (**4**) ($t_R$ 9.7 min, 2.3 mg) and (+)-oxanthromicin (**1**) ($t_R$ 11.4 min, 13.7 mg) (ESI Scheme S1†). Based on the above, the estimated % yield from the crude culture extract is **1** (0.99%), **2** (1.9%), **3** (0.71%), **4** (0.30%), **5** (0.14%), **6** (0.11%), **9** (0.15%) and **10** (2.1%) (Note: these yields do not take into account the transformation of **2** to **3** and **4**; **3** to **2**; **5** and **6** to **4** after HPLC purification). (ESI Fig. S13–S14†).

**(+)-Oxanthromicin (1)—**Yellow amorphous solid; $[\alpha]_D^{22} +157$ (*c* = 0.26, EtOH); UV (MeOH) $\lambda_{max}$ (log $\varepsilon$) 259 (4.34), 321 (4.31), 355 (4.22) nm; NMR (DMSO-$d_6$) see ESI Table S1 and Fig. S1a–S1b†; HRESI(−)MS *m*/*z* 653.1662 $[M - H]^-$ (calcd for $C_{36}H_{29}O_{12}^-$, 653.1664).

Author Manuscript Author Manuscript Author Manuscript Author Manuscript

**(±)-*hemi*-Oxanthromicin A (2)—**Yellow amorphous solid; $[\alpha]_D^{22}0$ (*c* = 0.10, EtOH); UV (MeOH) $\lambda_{max}$ (log $\varepsilon$) 259 (4.05), 325 (4.02), 341 (3.99), 356 (3.96) nm; NMR (DMSO-$d_6$) ESI Table S2 and Fig. S2a–S2b†; HRESI(−)MS *m*/*z* 327.0882 [M − H]$^-$ (calcd for $C_{18}H_{15}O_6^-$, 327.0874).

**(±)-*hemi*-Oxanthromicin B (3)—**Yellow amorphous solid; $[\alpha]_D^{22}0$ (*c* = 0.13, EtOH); UV (MeOH) $\lambda_{max}$ (log $\varepsilon$) 258 (4.12), 323 (4.10), 344 (4.04), 355 (4.03) nm; NMR (DMSO-$d_6$) ESI Table S3 and Fig. S3a–S3b†; HRESI(−)MS *m*/*z* 341.1029 [M − H]$^-$ (calcd for $C_{19}H_{17}O_6^-$, 341.1031).

**(±)-*spiro*-Oxanthromicin A (4)—**Yellow amorphous solid; $[\alpha]_D^{22}0$ (*c* = 0.13, EtOH); UV (MeOH) $\lambda_{max}$ (log $\varepsilon$) 239 (4.55), 258 (4.48), 303 (4.38), 356 (4.18) nm; NMR (DMSO-$d_6$) ESI Table S4 and Fig. S4a–S4b†; HRESI(−)MS *m*/*z* 617.1450 [M − H]$^-$ (calcd for $C_{36}H_{25}O_{10}^-$, 617.1453).

**(±)-*spiro*-Oxanthromicin B1 (5)—**UV (MeCN–$H_2O$) $\lambda_{max}$ 235, 275, 320, 360 nm; HRESI(−)MS *m*/*z* 649.1739 [M − H]$^-$ (calcd for $C_{37}H_{29}O_{11}^-$, 649.1715).

**(±)-*spiro*-Oxanthromicin B2 (6)—**UV (MeCN–$H_2O$) $\lambda_{max}$ 235, 275, 320, 360 nm; HRESI(−)MS *m*/*z* 649.1735 [M − H]$^-$ (calcd for $C_{37}H_{29}O_{11}^-$, 649.1715).

**(±)-*spiro*-Oxanthromicin C1 (7)—**UV (MeCN–$H_2O$) $\lambda_{max}$ 235, 275, 320, 360 nm; HRESI(−)MS *m*/*z* 635.1565 [M − H]$^-$ (calcd for $C_{36}H_{27}O_{11}^-$, 635.1559).

**(±)-*spiro*-Oxanthromicin C2 (8)—**UV (MeCN–$H_2O$) $\lambda_{max}$ 235, 275, 320, 360 nm; HRESI(−)MS *m*/*z* 635.1559 [M − H]$^-$ (calcd for $C_{36}H_{27}O_{11}^-$, 635.1559).

**Oxanthroquinone (9)—**Orange amorphous solid; UV (MeOH) $\lambda_{max}$ (log $\varepsilon$) 221 (4.19), 284 (4.14), 412 (3.53) nm; NMR (DMSO-$d_6$) ESI Table S5 and Fig. S5a–S5b†; HRESI(−)MS *m*/*z* 311.0568 [M − H]$^-$ (calcd for $C_{17}H_{11}O_6^-$, 311.0561).

## Chemical stability studies of 1–4

Aliquots of **1**–**4** (0.1 mg) were dissolved in either 0.1% TFA in MeCN (0.5 mL) or 0.1% TFA in MeOH (0.5 mL) and heated at 40 °C for 24 h, after which the solutions were analysed by HPLC-DAD-MS (Agilent Zorbax SB-$C_8$, 5 μm, 4.6 × 150 mm column, 15 min gradient elution at 1 mL min$^{-1}$ from 90% $H_2O$–MeCN to 100% MeCN with isocratic 0.05% formic acid modifier). Samples of **1**–**4** (0.1 mg) dissolved in MeOH (1.0 mL) were used as authentic standards, and analysed by the same HPLC method. Analytical results, as illustrated in the ESI Fig. S12–S14,† demonstrate that whereas **1** and **4** were stable under these conditions, **2** and **3** equilibrate, and transform through **5** and **6**, to **7** and **8**, and finally to **4**.

Author Manuscript Author Manuscript Author Manuscript Author Manuscript

## Synthetic studies

**2-Chloro-8-hydroxy-7-methylnaphthaquinone—**A solution of 2,4-dichloro-1,4-benzoquinone (354 mg, 2.00 mmol) and the Danishefsky diene derived from tiglic aldehyde[7] (340 mg, 2.18 mmol) in toluene (5 mL) was stirred at r.t. for 1 h. After concentrating *in vacuo*, the residue was dissolved in acetone and stirred at r.t. for 16 h in the presence of Jones reagent (2.5 M $CrO_3$ in 3.6 M $H_2SO_4$) (5.0 mL, 12.5 mmol). After quenching excess reagent by addition of 2-propanol (10 mL) the reaction mixture was filtered, extracted with $Et_2O$ (20 mL), and the organic phase washed with $H_2O$ (10 mL) and brine (10 mL). The residue recovered from concentrating *in vacuo* was recrystallised from EtOAc to afford 2-chloro-8-hydroxy-7-methylnaphthaquinone[8] (266 mg, 60% for 2 steps). $^1$H NMR (600 MHz, $CDCl_3$): $\delta_H$ = 12.06 (s, 1H), 7.56 (d, $J$ = 7.7 Hz, 1H), 7.53 (d, $J$ = 7.7 Hz, 1H), 7.17 (s, 1H), 2.37 (s, 3H).

**Oxanthroquinone ethyl ester (11)—**A solution of 2-chloro-8-hydroxy-7-methylnaphthaquinone (80 mg, 0.36 mmol) and the Danishefsky diene derived from ethyl diacetoacetate[9] (230 mg, 0.72 mmol) in toluene (5 mL) was refluxed for 3 days. After concentrating *in vacuo* the residue was extracted with $CH_2Cl_2$ (5 mL) and stirred in the presence of silica gel (240 mg) at r.t. for 5 min. The reaction mixture was then concentrated *in vacuo* and the residue purified by silica gel chromatography (isocratic elution 1 : 10 EtOAc–light petroleum) to afford oxanthroquinone ethyl ester (**11**) ($R_f$ 0.4; 71 mg, 58%). UV (MeOH) $\lambda_{max}$ (log $\varepsilon$) 221 (4.50), 273 (4.58), 414 (3.93) nm; $^1$H NMR (600 MHz, $CDCl_3$): $\delta_H$ = 13.28 (s, 1H), 10.49 (s, 1H), 7.78 (s, 1H), 7.69 (d, $J$ = 7.6 Hz, 1H), 7.49 (d, $J$ = 7.6 Hz, 1H), 4.53 (q, $J$ = 7.2 Hz, 1H), 2.99 (s, 3H), 2.38 (s, 3H), 1.48 (t, $J$ = 7.2 Hz, 3H); $^{13}$C NMR (150 MHz, DMSO-$d_6$): $\delta_C$ = 189.6, 181.6, 166.8, 160.0, 158.9, 141.0, 136.8, 136.5, 134.6, 130.2, 129.8, 122.4, 118.1, 115.7, 112.0, 61.5, 19.9, 15.9, 14.1 (ESI Fig. S6a–S6b[†]); HRESI (−)MS $m/z$ 339.0873 $[M - H]^-$ (calcd for $C_{19}H_{15}O_6^-$, 339.0874).

**Oxanthroquinone (9)—**A solution of **11** (70 mg, 0.21 mmol) in aq. LiOH (1 M; 2 mL) was stirred at 100 °C overnight. The dark red solution was then acidified by addition of aq. HCl (1 M; 2.1 mL) and extracted with $Et_2O$ (3 × 5 mL). The organic phase was dried over anhydrous $MgSO_4$, concentrated *in vacuo* and purified using a $C_{18}$ SPE cartridge (stepwise gradient of 90% $H_2O$–MeCN to 100% MeCN) to afford synthetic oxanthroquinone (**9**; 56 mg, 88%) identical in all respects to natural **9**.

**(±)-*hemi*-Oxanthromicin A (2)—**A solution of **9** (20 mg, 0.064 mmol) in anhydrous THF (1 mL) was cooled to 0 °C and MeMgBr (3 M in $Et_2O$; 430 μL, 1.3 mmol) was added. The mixture was allowed to reach r.t. and then stirred overnight. After quenching with sat. aqueous $NH_4Cl$, the reaction mixture was acidified to pH 4 with 0.1 M HCl and extracted with $Et_2O$ (3 × 3 mL), after which the organic phase was dried over anhydrous $MgSO_4$, concentrated *in vacuo*, and purified by semi-preparative HPLC [Agilent Zorbax Rx-$C_8$, 5 μm, 9.4 × 250 mm column, 15 min gradient elution at 3.5 mL $min^{-1}$ from 90% $H_2O$–MeCN to 100% MeCN with isocratic 0.01% TFA modifier] to afford synthetic (±)-*hemi*-oxanthromicin A (**2**; $t_R$ 10.9 min, 8.3 mg, 45%), identical in all respects to natural **2**, and recovered oxanthroquinone (**9**; $t_R$ 11.9 min, 9 mg, 43%).

Author Manuscript Author Manuscript Author Manuscript Author Manuscript

**3-*O*-Methyl oxanthroquinone ethyl ester (14)—**A solution of **11** (6.0 mg, 0.018 mmol) and $K_2CO_3$ (5.0 mg, 0.035 mmol) in acetone (1 mL) was treated with MeI (6.0 mg, 0.042 mmol) and stirred overnight at r.t. The filtered reaction mixture was acidified to pH 4 with 0.1 M HCl and extracted with $Et_2O$ (3 × 3 mL), and the organic phase dried over anhydrous $MgSO_4$, concentrated *in vacuo*, and purified by preparative HPLC [Phenomenex Luna $C_{18}$ (2), 10 μm, 21.2 × 250 mm column, 15 min gradient elution at 20 mL $min^{-1}$ from 90% $H_2O$–MeCN to 100% MeCN with isocratic 0.01% TFA modifier] to afford 3-*O*-methyl-oxanthroquinone ethyl ester (**14**; $t_R$ 16.9 min, 4.5 mg, 72%). UV (MeOH) $\lambda_{max}$ (log $\varepsilon$) 222 (4.70), 270 (4.72), 298 (4.28), 415 (3.94) nm; $^1$H NMR (600 MHz, $CDCl_3$): $\delta_H$ = 13.25 (s, 1H), 7.75 (s, 1H), 7.69 (d, $J$ = 7.7 Hz, 1H), 7.48 (d, $J$ = 7.7 Hz, 1H), 4.46 (q, $J$ = 7.2 Hz, 1H), 4.01 (s, 3H), 2.76 (s, 3H), 2.37 (s, 3H), 1.41 (t, $J$ = 7.2 Hz, 3H); $^{13}$C NMR (150 MHz, $CDCl_3$): $\delta_C$ = 190.3, 182.5, 167.3, 161.1, 160.0, 141.4, 137.8, 136.5, 135.8, 131.5, 130.6, 125.0, 118.8, 116.2, 107.6, 62.1, 56.6, 20.2, 16.5, 14.3 (ESI Fig. S7a–S7b†); HRESI(+)MS $m/z$ 377.0997 $[M + Na]^+$ (calcd for $C_{20}H_{18}O_6Na^+$, 377.0996).

**7-Desmethyloxanthroquinone ethyl ester (12)—**A solution of 3-bromojuglone[10] (100 mg, 0.40 mmol) and the Danishefsky diene derived from ethyl diacetoacetate[9] (250 mg, 0.79 mmol) in toluene (5 mL) was refluxed for 3 days. After concentrating *in vacuo* the residue was dissolved in $CH_2Cl_2$ (5 mL), stirred with silica gel (250 mg) at r.t. for 5 min, concentrated *in vacuo* and purified by silica gel chromatography (isocratic elution 1 : 10 EtOAc–light petroleum) to afford 7-desmethyloxanthroquinone ethyl ester (**12**; $R_f$ 0.4; 88 mg, 68%).[11] UV (MeOH) $\lambda_{max}$ (log $\varepsilon$) 220 (4.20), 272 (4.26), 409 (3.47) nm; $^1$H NMR (600 MHz, $CDCl_3$): $\delta_H$ = 12.93 (s, 1H), 10.53 (s, 1H), 7.79 (s, 1H), 7.78 (dd, $J$ = 7.5, 1.0 Hz, 1H), 7.62 (dd, $J$ = 8.3, 7.5 Hz, 1H), 7.31 (dd, $J$ = 8.3, 1.0 Hz, 1H), 4.54 (q, $J$ = 7.2 Hz, 1H), 2.99 (s, 3H), 1.48 (t, $J$ = 7.2 Hz, 3H); $^{13}$C NMR (150 MHz, $CDCl_3$): $\delta_C$ = 189.6, 182.2, 170.1, 163.6, 162.5, 148.0, 138.7, 135.8, 132.7, 125.0, 124.5, 121.2, 118.9, 117.5, 115.1, 62.9, 21.9, 14.1 (ESI Fig. S8a–S8b†); HRESI(−)MS $m/z$ 325.0719 $[M - H]^-$ (calcd for $C_{18}H_{13}O_6^-$, 325.0718).

**7-Desmethyloxanthroquinone (13)—**A solution of **12** (48 mg, 0.15 mmol) in aq. LiOH (1 M; 1 mL) was stirred at 100 °C overnight. The dark red solution was acidified by aq. HCl (1 M; 1.05 mL) and extracted with $Et_2O$ (2 × 5 mL), after which the organic phase was dried over anhydrous $MgSO_4$, concentrated *in vacuo*, and purified using a $C_{18}$ SPE cartridge (stepwise gradient of 90% $H_2O$–MeCN to 100% MeCN) to afford 7-desmethyloxanthroquinone (**13**; 39 mg, 90%).[12] UV (MeOH) $\lambda_{max}$ (log $\varepsilon$) 217 (4.68), 280 (4.72), 411 (4.08) nm; $^1$H NMR (600 MHz, DMSO-$d_6$): $\delta_H$ = 12.89 (s, 1H), 7.76 (dd, $J$ = 8.3, 7.5 Hz, 1H), 7.66 (dd, $J$ = 7.5, 1.1 Hz, 1H), 7.60 (s, 1H), 7.36 (dd, $J$ = 8.3, 1.1 Hz, 1H), 2.71 (s, 3H); $^{13}$C NMR (150 MHz, DMSO-$d_6$): $\delta_C$ = 189.4, 182.1, 168.3, 161.5, 159.2, 140.9, 136.4, 136.2, 132.5, 131.2, 124.5, 122.5, 118.4, 116.9, 112.2, 20.0 (ESI Fig. S9a–S9b†); HRESI(−)MS $m/z$ 297.0405 $[M - H]^-$ (calcd for $C_{16}H_9O_6^-$, 297.0405).

## K-Ras bioassay

Madin-Darby canine kidney (MDCK) cells stably co-expressing monomeric green fluorescent protein (mGFP) coupled to the N-terminus of oncogenic K-Ras (K-RasG12 V) and mCherry- CAAX, a red fluorescent fusion protein that decorates endomembranes,[4] were

Author Manuscript Author Manuscript Author Manuscript Author Manuscript

plated at 150 000 cells per well on 12-well plates. After 24 h, cells were treated with compounds and incubated for another 48 h. Each compound was tested in 3 independent experiments. At the end of incubation time, cells were fixed with 4% paraformaldehyde and imaged in a Nikon A1R confocal microscope. Ras mislocalisations from the plasma membranes were calculated using Manders coefficients, by measuring the fraction of mCherry-CAAX co-localizing with mGFP-K-RasG12 V.[4] $IC_{50}$ values and two-tailed *t*-tests were calculated using Prism software (Ver. 5.0c, GraphPad). $E_{max}$ quantifies the maximum extent of mislocalisation of K-Ras from the plasma membrane to endomembrane.

## Supplementary Material

Refer to Web version on PubMed Central for supplementary material.

## Acknowledgments

We acknowledge the assistance of A. Crombie (MST) in the fermentation and genetic sequencing of isolates, and A. Lacey (MST) in the extraction and purification of metabolites. This research was funded in part by the Australian Research Council (ARC DP120100183 and LP120100088), The University of Queensland, the Institute for Molecular Bioscience, and the Cancer Prevention and Research Institute of Texas (RP100483).

## Notes and references

1. Hancock JF. Nat Rev Mol Cell Biol. 2003; 4:373. [PubMed: 12728271]
2. Bodemann BO, White MA. Curr Biol. 2013; 23:R17. [PubMed: 23305663]
3. Baines AT, Xu D, Der CJ. Future Med Chem. 2011; 3:1787. [PubMed: 22004085]
4. Cho, K-j, Park, J-H., Piggott, AM., Salim, AA., Gorfe, AA., Parton, RG., Capon, RJ., Lacey, E., Hancock, JF. J Biol Chem. 2012; 287:43573. [PubMed: 23124205]
5. (a) Patel M, Horan AC, Gullo VP, Loebenberg D, Marquez JA, Miller GH, Waitz JA. J Antibiot. 1984; 37:413. [PubMed: 6725146] (b) Wright JJK, Merill Y, Puar MS, mcPhail AT. J Chem Soc, Chem Commun. 1984:473.
6. Becker HD, Sanchez D. J Org Chem. 1979; 44:1787.
7. Gieseler MT, Kalesse M. Org Lett. 2011; 13:2430. [PubMed: 21473644]
8. Boisvert L, Brassard P. J Org Chem. 1988; 53:4052.
9. Caron B, Brassard P. Tetrahedron. 1993; 49:771.
10. Tietze LF, Singidi RR, Gericke KM. Chem – Eur J. 2007; 13:9939. [PubMed: 17886848]
11. Bingham SJ, Tyman JHP. J Chem Soc, Perkin Trans. 1997; 1:3637.
12. Lee TS, Das A, Khosla C. Bioorg Med Chem. 2007; 15:5207. [PubMed: 17524653]

Author Manuscript Author Manuscript Author Manuscript Author Manuscript

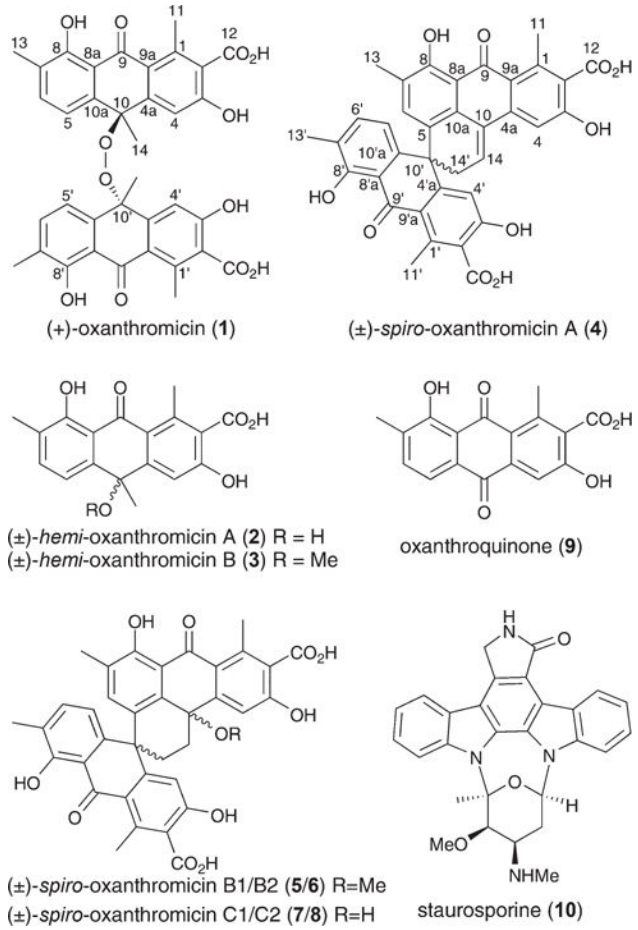


**Fig. 1.**
Structures of **1–10**.

Author Manuscript Author Manuscript Author Manuscript Author Manuscript

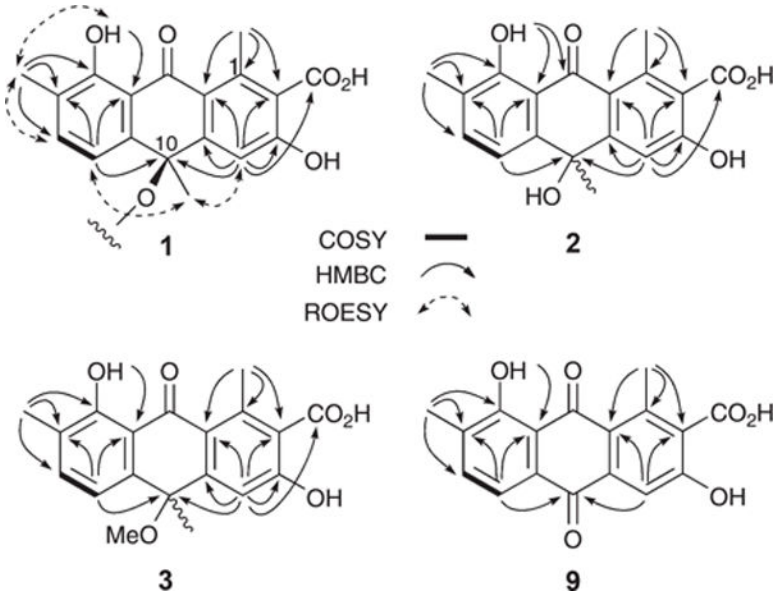


**Fig. 2.**
Selected 2D NMR correlations for **1–3** and **9**.

Author Manuscript Author Manuscript Author Manuscript Author Manuscript

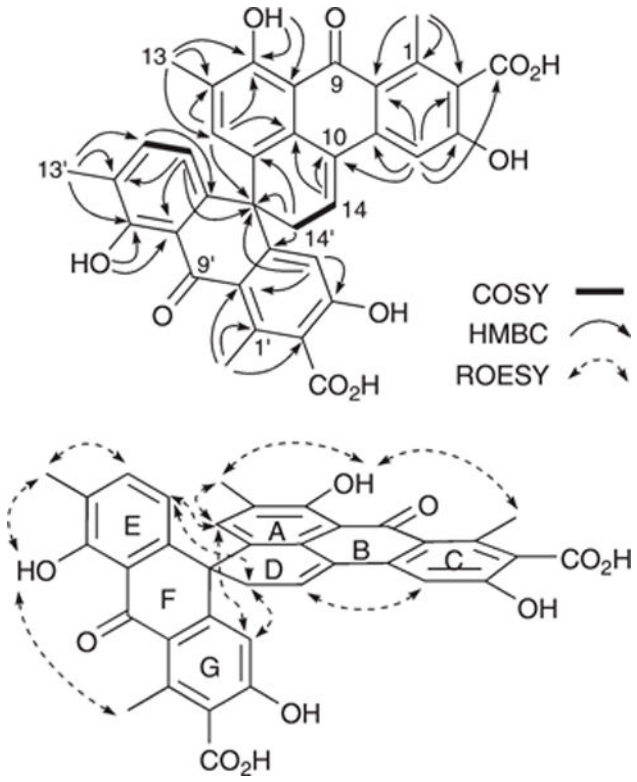


**Fig. 3.**
Selected 2D NMR correlations for **4**.

Author Manuscript Author Manuscript Author Manuscript Author Manuscript

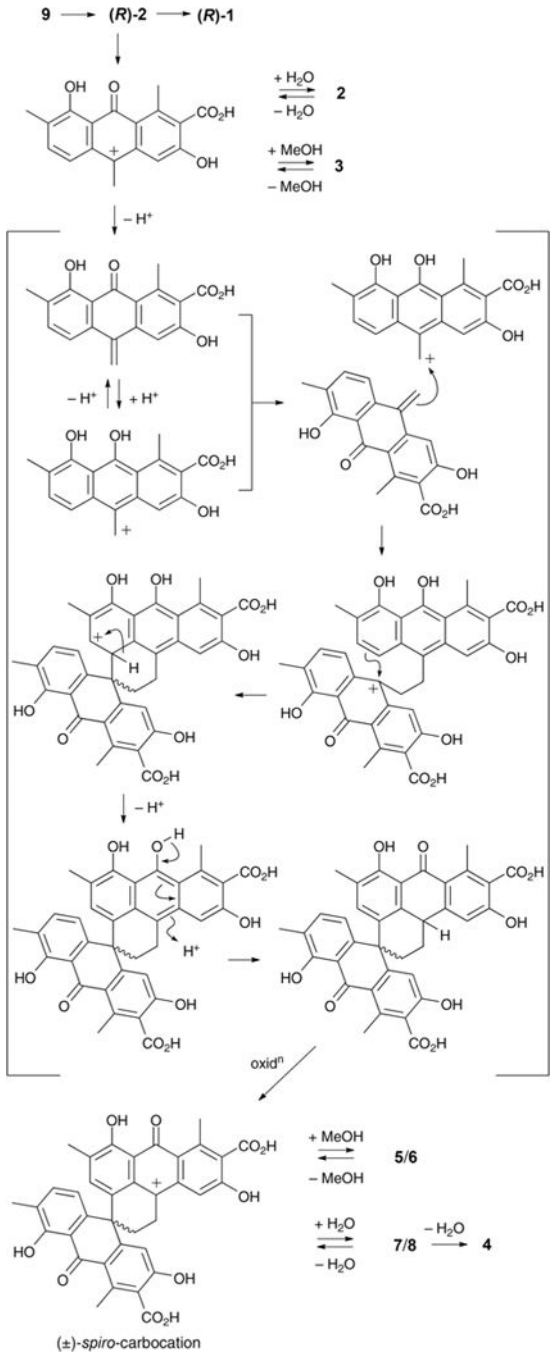


**Fig. 4.**
Biosynthetic/chemical pathway linking **1–9**.

Author Manuscript Author Manuscript Author Manuscript Author Manuscript

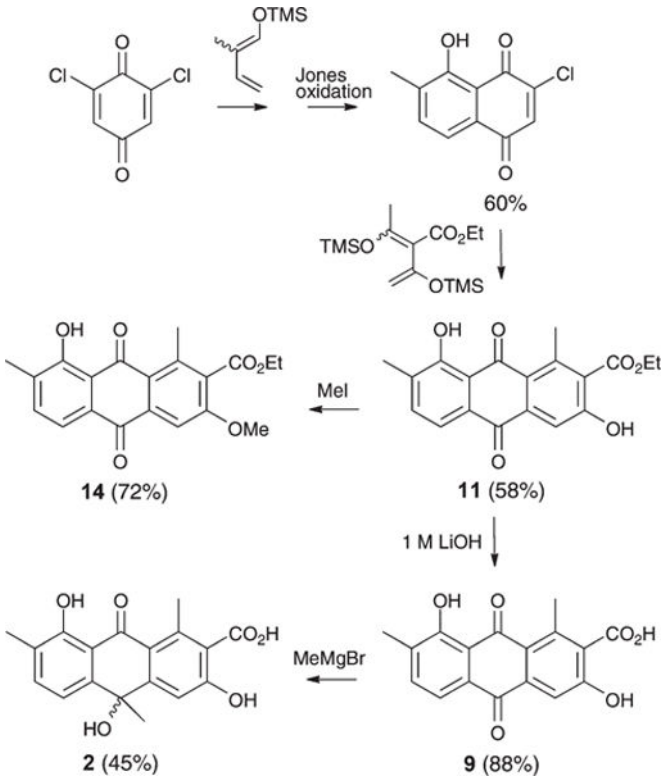


**Scheme 1.**
Synthesis of **2**, **9**, **11**, and **14**.

Author Manuscript Author Manuscript Author Manuscript Author Manuscript

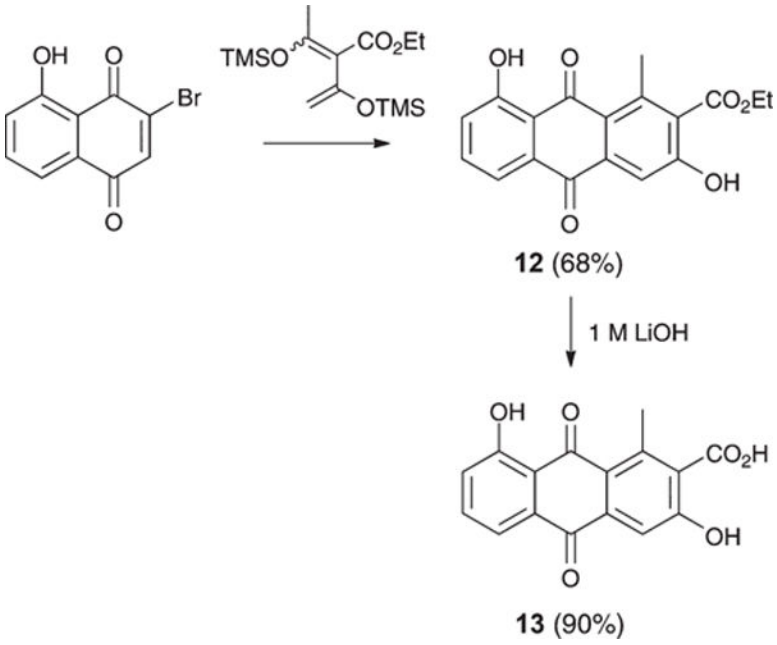


**Scheme 2.**
Synthesis of **12** and **13**.

Author Manuscript

Author Manuscript

Author Manuscript

Author Manuscript

## Table 1

Summary of K-Ras mislocalisation studies

| Compound | $E_{max}$ ± SEM | $IC_{50}$ (μM) ± SEM |
|---|---|---|
| **1** | 0.76 ± 0.02 | 62.5 ± 8.0 |
| **2** | 0.47 ± 0.03 | *a* |
| **4** | 0.75 ± 0.03 | 26.7 ± 7.2 |
| **9** | 0.44 ± 0.05 | *a* |
| **11** | 0.76 ± 0.04 | 4.6 ± 0.8 |
| **12** | 0.73 ± 0.02 | 18.6 ± 2.9 |
| **13** | 0.43 ± 0.02 | *a* |
| **14** | 0.73 ± 0.02 | 1.2 ± 0.3 |
| **10** | 0.67 ± 0.03 | 0.00051 ± 0.0002 |

[a]Compounds with an $E_{max} < 0.50$ were deemed to be inactive. Negative control DMSO $E_{max} = 0.37$.